Journal of Sound and Vibration (2000) **234**(1), 67–83
doi:10.1006/jsvi.1999.2854, available online at http://www.idealibrary.com on IDEAL®

COUPLED TORSIONAL AND BENDING VIBRATIONS OF ACTIVELY CONTROLLED DRILLSTRINGS

A. S. YIGIT AND A. P. CHRISTOFOROU

Department of Mechanical and Industrial Engineering, Kuwait University, P. O. Box 5969, *Safat* 13060, *Kuwait*

(*Received* 23 *March* 1999, *and in final form* 30 *November* 1999)

The dynamics of actively controlled drillstrings is studied. The equations of motion are derived using a lumped parameter model in which the coupling between torsional and bending vibrations is considered. The model also includes the dynamics of the rotary drive system which contains the rotary table, the gearbox and an armature controlled DC motor. The interactions between the drillstring and the borehole which are considered, include the impacts of collars with the borehole wall as well as bit rotation-dependent weight and torque on bit (WOB and TOB). Simulation results obtained by numerically solving the equations of motion are in close qualitative agreement with field and laboratory observations regarding stick–slip oscillations. A linear quadratic regulator (LQR) controller is designed based on a linearized model and is shown to be effective in eliminating this type of oscillations. It is also shown that for some operational parameters the control action may excite large bending vibrations due to coupling with the torsional motion.

1. INTRODUCTION

Drilling deep wells for oil or gas production is carried out by a rotary drilling system. The essential components of such a system is shown in Figure 1. The drill bit is driven by a drive

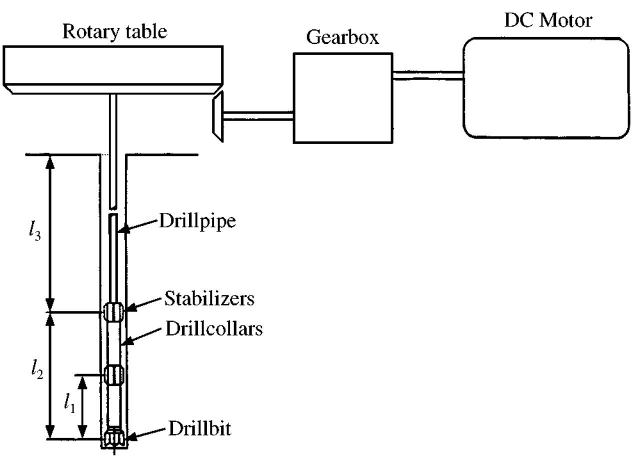

Figure 1. A sketch of the drillstring with the rotary table drive system.

system at the surface, mostly an electric motor with a gearbox and a rotary table. The drillstring transmits torque from the drive system to the bit and consists mainly of slender tubes called drill pipes. The lowest part of the drillstring is under compression and to avoid buckling it consists of thick-walled tubes, called drill collars [1].

Drillstring vibrations have been studied extensively in recent years [1–8]. Axial, bending and torsional vibrations are all known to be present and coupled. Phenomena such as bit bounce, stick–slip, forward and backward whirl and parametric instabilities have all been shown to occur. These vibrations, particularly stick–slip oscillations, are detrimental to the life of the drillstring and the downhole equipment. Large cyclic stresses induced by this type of motion can lead to fatigue problems. In addition, the high bit speed level in the slip phase can excite severe axial and lateral vibrations in the bottom hole assembly, which may cause excessive bit wear and reduction in the penetration rate [9]. Clearly, it is very desirable that these vibrations are controlled and minimized in order to achieve efficient and smooth drilling operations.

Various methods for controlling drillstring torsional vibrations have been proposed [4, 10–14]. These methods include operational guidelines to avoid, eliminate or reduce torsional vibrations as well as active control methods using feedback. Brett [4], proposed to use speed feedback in addition to employing an overrunning clutch to control drillstring torsional vibrations. Halsey *et al.* [10], showed that torque feedback can help eliminate stick–slip vibrations. Sananikone *et al.* [11] designed a feedback system that uses motor current and acceleration signals, and compared the performance with torque feedback only and motor current feedback only strategies. They concluded that current and acceleration feedback perform very well in suppressing torsional vibrations. Jansen *et al.* [12], proposed an active control system to be used with a hydraulic top drive. The control was designed in the Laplace domain and used pressure fluctuation measurements. A similar controller was shown to work in the case of a DC motor driven system [13]. Recently, Serrarens *et al.* [14], used H_∞ control which takes uncertainties and varying parameters into account to successfully suppress stick–slip oscillations. Although most proposed control methods have been shown to be successful in controlling torsional vibrations, the effects of this control on bending vibrations have not been studied. In order to design and implement an effective control system, a coupled model is essential for identifying the critical speeds as well as predicting the behaviour of the whole system [15]. In other words, the effect of controlling torsional vibrations on the bending vibrations should also be examined. Recently, the authors proposed a model which considers the full coupling between torsional and lateral vibrations, where the excitation at the bit is assumed to be related to the rotation of the bit [16]. This makes the coupling between torsional and bending vibrations much stronger and nonlinear. The results showed that torsional vibrations can significantly affect the dynamic behavior, especially when they escalate into stick–slip oscillations. The findings were in qualitative agreement with laboratory and field observations [4, 10]. In the current paper, this model is extended to include the effects of the rotary table drive system and control (see Figure 1). The Torque-on-Bit (TOB) expression is also improved by including the speed dependence in the model. Finally, simulations show that the proposed model is quite realistic with respect to stick–slip oscillations, which are effectively eliminated through an optimal state feedback control scheme. However, the effect of control on the lateral vibrations may be significant, and care must be taken in selecting the operating parameters.

2. EQUATIONS OF MOTION

The equations of motion for coupled torsional and bending vibrations of an actively controlled drillstring are obtained by using a simplified lumped parameter model. The

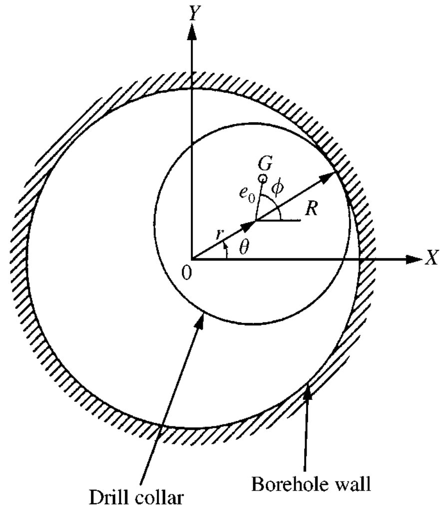

Figure 2. Cross-sectional view of a deflected drill collar section inside the borehole.

necessary geometry used for the model is shown in Figure 2. The first three of the equations shown below were originally developed in reference [16] assuming a prescribed rotary table speed. It is more realistic, however, to include the rotary table drive system including the motor dynamics. Here, it is assumed that the rotary table is driven by an armature-controlled DC motor. The resulting complete equations are given as

$$(m + m_f)(\ddot{r} - r\dot{\theta}^2) + k(\phi, \dot{\phi})r + c_h|\mathbf{v}|\dot{r} = (m + m_f)e_0[\dot{\phi}^2 \cos(\phi - \theta) + \ddot{\phi}\sin(\phi - \theta)] - F_r, \quad (1)$$

$$(m + m_f)(r\ddot{\theta} + 2\dot{r}\dot{\theta}) + c_h|\mathbf{v}|r\dot{\theta} = (m + m_f)e_0[\dot{\phi}^2 \sin(\phi - \theta) - \ddot{\phi}\cos(\phi - \theta)] + F_\theta, \quad (2)$$

$$J\ddot{\phi} + k_T(\phi - \phi_{rt}) + c_v\dot{\phi} + c_h|\mathbf{v}|\dot{r}e_0 \sin(\phi - \theta) - c_h|\mathbf{v}|r\dot{\theta}e_0 \cos(\phi - \theta)$$

$$= -T(\phi, \dot{\phi}) + F_\theta[R - e_0 \cos(\phi - \theta)] - F_r e_0 \sin(\phi - \theta), \quad (3)$$

$$(J_{rt} + n^2 J_m)\ddot{\phi}_{rt} + k_T(\phi_{rt} - \phi) + c_{rt}\dot{\phi}_{rt} - nT_m = 0, \quad (4)$$

$$L\dot{I} + RI + V_b = V_c, \quad (5)$$

where ϕ_{rt} is the angular displacement at the rotary table (top of the drillstring), ϕ is the angle of rotation of the drill collars, $\mathbf{v}$ is the velocity of the geometric center of the drill collar section, e_0 is the eccentricity of the center of mass with respect to the geometric center of the collar section, R is the radius of the drill collars, J, m, m_f, $k(\phi, \dot{\phi})$, k_T, c_h and c_v are the equivalent mass moment of inertia, mass, added fluid mass, transverse stiffness, torsional stiffness, hydrodynamic and viscous damping coefficients which are derived from the associated continuous model of the drillstring by using a Lagrangian approach. In this approach, the stabilized section of the drill collars is modelled as a simply supported beam for transverse motion of the collars, and the whole drillstring is assumed to be fixed at the top, and free at the bit for torsional motion. The drill collars are assumed to be rigid for torsional vibrations, in other words, the torsional deformations are assumed to take place only in the drill pipe. This assumption is justified since the drillcollars are much stiffer than the drill pipe in torsion [13]. Assuming one-mode approximation for both the transverse and torsional vibrations, the equivalent system parameters are obtained as

$$J = 2\rho I_a l_2 + (1/3)\rho I_p l_3, \tag{6}$$

$$m = \rho\pi(d_o^2 - d_i^2)l_1/8, \tag{7}$$

$$m_f = \pi\rho_f(d_i^2 + C_a d_o^2)l_1/8, \tag{8}$$

$$k(\phi, \dot{\phi}) = \frac{EI_a\pi^4}{2l_1^3} - \frac{T(\phi, \dot{\phi})\pi^3}{2l_1^2} - \frac{F(\phi)\pi^2}{2l_1}, \qquad k_T = \frac{GI_p}{l_3}, \tag{9, 10}$$

$$c_h = \frac{2}{3\pi}\rho_f C_d d_o l_1, \tag{11}$$

$$c_v = \frac{\pi\mu_f d_o^3 l_2}{2(d_h - d_o)}, \tag{12}$$

where ρ, E and G are the density, Young's modulus, and shear modulus of the drillstring material, respectively, $I_a = \pi(d_o^4 - d_i^4)/64$ is the area moment of inertia for the collar cross-section, d_o and d_i are the outside and inside diameters of the drill collars, respectively, ρ_f and μ_f are the density and the viscosity of the drilling mud, C_a is the added mass coefficient due to the displayed mass of the mud inside the drillstring, C_d is the drag coefficient for the hydrodynamic damping due to the mud, d_h is the borehole diameter, $I_p = \pi(\bar{d}_o^4 - \bar{d}_i^4)/32$ is the polar area moment of inertia of the drill pipe section, $\bar{d}_o$ and $\bar{d}_i$ are the outside and inside diameters of the drill pipe respectively.

J_{rt} and J_m are the inertia of the rotary table and the drive motor, respectively, n is the gear ratio, and c_{rt} is the equivalent viscous damping in the drive system. I is the motor current, L and R are the inductance and resistance of the DC motor driving the rotary table, V_c is the voltage applied to the motor and T_m is the drive torque applied at the motor shaft and it is given as

$$T_m = K_m I, \tag{13}$$

where K_m is the motor constant. The back electromotive (emf) force V_b is given as

$$V_b = K_m n\dot{\phi}_{rt}. \tag{14}$$

The torque on bit (TOB), $T(\phi, \dot{\phi})$, and the weight on bit (WOB), $F(\phi)$ are assumed to be given as

$$T(\phi, \dot{\phi}) = (T_0 + T_f \sin n_b\phi)f(\dot{\phi}), \tag{15}$$

$$F(\phi) = F_0 + F_f \sin n_b\phi, \tag{16}$$

where n_b is the bit factor which depends on the type of the bit used, and, the subscripts 0 and f denote the mean and the amplitude values respectively. The dependence of the TOB and WOB on the bit angular displacement, ϕ, was initially proposed by the authors [16] as an extension of harmonic functions of time used in earlier studies. Although this assumption has provided some insight towards understanding the nature of stick–slip oscillations, it was incomplete since the effect of bit speed was not included. This effect is supported by experimental evidence which shows that the amplitude of the torque is a function of bit speed with the friction torque being larger at low speeds [4]. Various functions have been used to model this dependence [13, 17]. In this study, a continuous function of $\dot{\phi}$ is used to represent the effect of the bit speed on the bit torque and it is given as [17]

$$f(\dot{\phi}) = \tanh \dot{\phi} + \frac{\alpha_1 \dot{\phi}}{(1 + \alpha_2 \dot{\phi}^2)}, \tag{17}$$

where the constant parameters α_1 and α_2 determine the transition from static to kinetic friction regions. They are selected as $\alpha_1 = 2$ and $\alpha_2 = 1$ to match the experimental data.

With these TOB and WOB models, the bit/formation interactions are now expressed as functions of motion. As a consequence, linear phenomena such as whirling [1], and simple and parametric resonance [5], which are based on the assumption of harmonic excitations, are no longer straightforward. Other intermittent external excitations are F_r and F_θ which are the radial and transverse contact forces, respectively, resulting from impacts of the drill collars with the borehole wall. When there is no contact between the collars and the borehole wall, these forces are zero. The impacts are accounted for by using the momentum balance method with appropriate coefficients of restitution and friction. The impact model is capable of capturing both rolling with and without slip of the drill collars along the borehole wall and is given in detail in reference [16]. The momentum balance equations used for the impact model are developed in the next section.

3. ANALYSIS OF CONTACT WITH THE BOREHOLE WALL

In most previous studies, the impact between the drill collars and the borehole wall was modelled through a linear or Hertzian contact stiffness [1, 7], and the effect of friction was accounted for by assuming continuous sliding between the two surfaces. Clearly, there might be situations where the collars roll along the borehole wall without slip. Recently, the authors [16] used the momentum balance method which is based on the assumption that the impact is instantaneous [18]. In this study, the same impact model is used, for which a brief explanation follows.

The impulse-momentum equations are obtained by integrating equations (1)–(5) with respect to time during the contact duration $\Delta t = t_2 - t_1$.

$$\int_{t_1}^{t_2} \{(m + m_f)(\ddot{r} - r\dot{\theta}^2) + k(\phi, \dot{\phi})r + c_h|\mathbf{v}|\dot{r}\}\,\mathrm{d}t$$

$$= \int_{t_1}^{t_2} \{(m + m_f)e_0[\dot{\phi}^2 \cos(\phi - \theta) + \ddot{\phi} \sin(\phi - \theta)] - F_r\}\,\mathrm{d}t, \tag{18}$$

$$\int_{t_1}^{t_2} \{(m+m_f)(r\ddot{\theta}+2\dot{r}\dot{\theta})+c_h|\mathbf{v}|r\dot{\theta}\}\,\mathrm{d}t$$

$$=\int_{t_1}^{t_2} \{(m+m_f)e_0[\dot{\phi}^2\sin(\phi-\theta)-\ddot{\phi}\cos(\phi-\theta)]+F_\theta\}\,\mathrm{d}t, \tag{19}$$

$$\int_{t_1}^{t_2} \{J\ddot{\phi}+k_T(\phi-\phi_{rt})+c_v\dot{\phi}+c_h|\mathbf{v}|\dot{r}e_0\sin(\phi-\theta)-c_h|\mathbf{v}|r\dot{\theta}e_0\cos(\phi-\theta)\}\,\mathrm{d}t$$

$$=\int_{t_1}^{t_2} \{-T(\phi)+F_\theta[R-e_0\cos(\phi-\theta)]-F_re_0\sin(\phi-\theta)\}\,\mathrm{d}t, \tag{20}$$

$$\int_{t_1}^{t_2} \{(J_{rt}+n^2J_m)\ddot{\phi}_{rt}+k_T(\phi_{rt}-\phi)+c_{rt}\dot{\phi}_{rt}-nT_m\}\,\mathrm{d}t=0 \tag{21}$$

$$\int_{t_1}^{t_2} \{L\dot{I}+RI+V_b-V_c\}\,\mathrm{d}t=0. \tag{22}$$

Noting that the system configuration is continuous, if the contact duration is assumed to approach zero, equations (18)–(22) can be shown to yield the momentum balance equations [18]:

$$(m+m_f)\Delta\dot{r}=-P_r+(m+m_f)e_0\Delta\dot{\phi}\sin(\phi-\theta), \tag{23}$$

$$(m+m_f)r\Delta\dot{\theta}=P_\theta-(m+m_f)e_0\Delta\dot{\phi}\cos(\phi-\theta), \tag{24}$$

$$J\Delta\dot{\phi}=[R-e_0\cos(\phi-\theta)]P_\theta-e_0\sin(\phi-\theta)P_r, \tag{25}$$

$$(J_{rt}+n^2J_m)\Delta\dot{\phi}_{rt}=0, \tag{26}$$

where $\Delta\dot{r}$, $\Delta\dot{\theta}$, $\Delta\dot{\phi}$ and $\Delta\dot{\phi}_{rt}$ are the jump discontinuities in the velocities, and P_r and P_θ are the impulses in radial and transverse directions, respectively, defined as

$$P=\lim_{\Delta t\to 0}\int_{t_1}^{t_2} F(t)\,\mathrm{d}t. \tag{27}$$

The radial and transverse impulse values for a particular impact are calculated using the two-dimensional rigid-body impact-friction model proposed by Wang and Mason [19]. For details of this model the readers are referred to references [16, 19].

The response of the system before an impact is obtained by numerical integration of the equations of motion (equations (1)–(5)). At each integration time step, the contact conditions are checked using a contact algorithm. If an impact is detected to occur, the integration is stopped and the momentum balance equations (equations (23)–(26)) are formed and solved for the jump discontinuities in velocities. Then, the integration is restarted again with the new initial conditions.

4. CONTROL DESIGN

In control design a linear model is preferred. Such a model can be obtained by linearizing the governing equations (1)–(5). In this case, the lateral motion becomes uncontrollable with the drive motor, and need not be included in the model. Thus, the following set of equations represent the reduced order linear model which can be used for control design:

$$J\ddot{\phi} + k_T(\phi - \phi_{rt}) + c_v\dot{\phi} = 0, \tag{28}$$

$$(J_{rt} + n^2 J_m)\ddot{\phi}_{rt} + k_T(\phi_{rt} - \phi) + c_{rt}\dot{\phi}_{rt} - nK_m I = 0, \tag{29}$$

$$L\dot{I} + RI + K_m n\dot{\phi}_{rt} = V_c. \tag{30}$$

It should be noted that the reduced order model is only used to design a linear controller. The resulting control is then applied to the full model to evaluate the performance of the proposed controller. It is also worth noting that since the reduced order model does not contain the equations for lateral motion, it is difficult to predict the performance of the controller when applied to the real system without running a full simulation or a real test. In fact, it is one of the objectives of this paper to show the effect of this type of controllers on the lateral motion of drillstrings.

In order to facilitate the control design, the equations of motion for the reduced order model are re-written in state space form as

$$\dot{\mathbf{x}} = \mathbf{A}\mathbf{x} + \mathbf{B}V_c, \tag{31}$$

where $\mathbf{x}$ is the state vector defined as

$$\mathbf{x}^{\mathrm{T}} = [(\phi - \phi_{rt}) \;\; \phi_{rt} \;\; \dot{\phi}_{rt} \;\; \dot{\phi} \;\; I], \tag{32}$$

where $()^{\mathrm{T}}$ denotes matrix transpose. $\mathbf{A}$ and $\mathbf{B}$ are the state and input matrices, respectively, and given by

$$\mathbf{A} = \begin{bmatrix} 0 & 0 & -1 & 1 & 0 \\ 0 & 0 & 1 & 0 & 0 \\ K_T/(J_{rt} + n^2 J_m) & 0 & -c_{rt}/(J_{rt} + n^2 J_m) & 0 & nK_m/(J_{rt} + n^2 J_m) \\ -K_T/J & 0 & 0 & -c_v/J & 0 \\ 0 & 0 & -K_m n/L & 0 & -R/L \end{bmatrix}, \tag{33}$$

$$\mathbf{B}^{\mathrm{T}} = [0 \;\; 0 \;\; 0 \;\; 0 \;\; 1/L]. \tag{34}$$

The problem can then be considered as a set point control problem where the objective is to bring all the states to their desired levels within a prescribed period of time when the states are disturbed by an external influence (e.g., bit torque).

The system $(\mathbf{A}, \mathbf{B})$ can be verified to be controllable by showing that the controllability matrix is of full rank. A linear quadratic Regulator (LQR) controller can then be designed which minimizes the following performance index:

$$C = \frac{1}{2}\int_0^\infty (\mathbf{x}^{\mathrm{T}}\mathbf{Q}\mathbf{x} + rV_c^2)\,\mathrm{d}t, \tag{35}$$

where $\mathbf{Q}$ is a weighting matrix which is chosen to reflect the relative importance of each state and r is a weighting factor to adjust the control effort. This controller is selected because it allows the designer to have a balance between the closed-loop performance and the required control effort. A close look at the quadratic performance index would reveal that it is related (not equal) to the total electromechanical energy in the system (the displacement terms are related to the elastic potential energy, the velocity terms are related to kinetic energy and the current term is related to the electrical energy). Basically, a weighted sum of square of the state error and the control energy required is being minimized with this performance index. The entries of the weighting matrix as well as the parameter r are used as tuning parameters to obtain the desired response.

The resulting optimal control voltage is given by [20]

$$V_c = V_{ref} - \mathbf{K}(\mathbf{x} - \mathbf{x}_d), \tag{36}$$

where $\mathbf{x}_d$ is the desired state vector, and $\mathbf{K}$ is the gain matrix given as

$$\mathbf{K} = \frac{1}{r}\mathbf{B}^{\mathrm{T}}\mathbf{P}, \tag{37}$$

where $\mathbf{P}$ is the symmetric, positive-definite solution matrix of the algebraic Riccati equation given by

$$\mathbf{A}^{\mathrm{T}}\mathbf{P} + \mathbf{P}\mathbf{A} - \frac{1}{r}\mathbf{P}\mathbf{B}\mathbf{B}^{\mathrm{T}}\mathbf{P} + \mathbf{Q} = \mathbf{0}. \tag{38}$$

The control voltage necessary to keep the torsional vibrations zero while maintaining a desired bit and rotary table speed is given by

$$V_c = V_{ref} - K_1(\phi - \phi_{rt}) - K_2(\phi_{rt} - \omega_d t) - K_3(\dot{\phi}_{rt} - \omega_d) - K_4(\dot{\phi} - \omega_d) - K_5 I, \tag{39}$$

where V_{ref} is a constant reference voltage applied to maintain the desired speed, ω_d at steady state in the absence of any disturbance and given by

$$V_{ref} = K_m n \omega_d. \tag{40}$$

It is important to examine each term in the control equation. The first term is the open-loop voltage to be applied in case no feedback is used. The second term is essentially a torque feedback since the measured torque at the rotary table shaft is $k_T(\phi - \phi_{rt})$. The third and the fourth terms are classical integral and proportional feedback terms applied to the rotary speed (PI control), the fifth term is the bit speed feedback, and the last term represents the current feedback. Except for the bit speed, all other quantities in the control can easily be measured or determined. The bit speed measurement requires downhole equipment and may be the most challenging task. It is becoming a common practice, however, to use an instrumented bit which makes this measurement possible. Even in the absence of such measurements, a state estimator can be designed to estimate the bit speed from the other measurements since it is observable through the other states.

At this point, it is worth mentioning that the optimal control designed based on the linear reduced order model, will not remain optimal with respect to the performance index used. Consequently, some performance degradation should be expected when this controller is implemented in a real situation. Therefore, simulations with full model are carried out to show that the results are satisfactory for the operating conditions considered. This is especially important since the lateral motion is non-linearly coupled to the linear dynamic model used in designing the controller.

5. SIMULATION RESULTS AND DISCUSSION

The parameters used in the following simulations are shown in Table 1, and represent a typical case in oil well drilling operations. The desired rotary table speed is chosen as 11·6 rad/s (110 r.p.m.) or 15 rad/s (145 r.p.m.) which are within the common operating range for oil well drilling. From a simple linear and uncoupled analysis for this set-up, the critical frequency for torsional resonance is found to be 1·85 rad/s, while the critical frequency for whirling resonance (due to bending) is found to be 6·14 rad/s. It is assumed that the rotary table and the bit are rotating at the desired speed when the bit is off bottom. When the bit starts to interact with the formation the system will inevitably be disturbed with the possibility of torsional and bending vibrations. The control objective is to bring the table speed back to the desired speed while minimizing these vibrations.

Figures 3–6 show the response in the absence of any feedback control. Though the rotary table speed does not change appreciably, significant stick–slip behavior is seen at the bit.

TABLE 1

Parameters used in the simulations

Drillstring	*Drilling mud*
$E = 210$ GPa	$\rho_f = 1500$ kg/m^3
$\rho = 7850$ kg/m^3	$C_d = 1$
$d_o = 0{\cdot}2286$ m	$C_a = 1{\cdot}7$
$d_i = 0{\cdot}0762$ m	$\mu_f = 0{\cdot}2$ N s/m^2
$e_0 = 0{\cdot}0127$ m	
$l_1 = 19{\cdot}81$ m,	*Borehole*
$l_2 = 200$ m	$E = 210$ GPa
$l_3 = 2000$ m	$\rho = 7850$ kg/m^3
$\bar{d}_o = 0{\cdot}127$ m,	$d_h = 0{\cdot}4286$ m
$\bar{d}_i = 0{\cdot}095$ m	
Rotary Drive System	
$J_{rt} = 930$ kg m^2	$R = 0{\cdot}01\ \Omega$
$J_m = 23$ kg m^2	$L = 0{\cdot}005$ H
$c_{rt} = 0$	$K_m = 6$ V s
$n = 7{\cdot}2$	
Weight and torque on bit	
$P_0 = 100$ kN, $P_f = 50$ kN;	$T_0 = 4$ kN m, $T_f = 2$ kNm

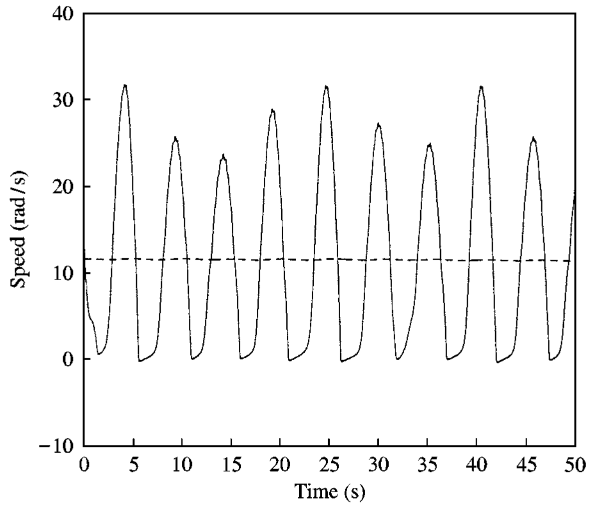

Figure 3. Stick–slip oscillations as seen in the bit and table speeds. ——, bit speed; – – –, table speed.

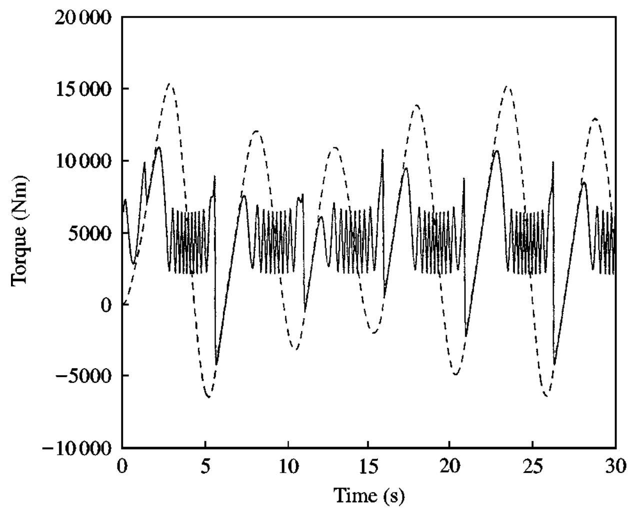

Figure 4. Stick–slip oscillations as seen in the bit and top torques. ——, bit torque; – – –, top torque.

The bit momentarily stops causing the TOB and the top torque to reach very high values. The bit may even spin backwards for short intervals of time causing negative values of TOB as seen in Figures 3 and 4 which are in close qualitative agreement with the field measurements [10, 13]. When the bit starts slipping, the energy stored in the drillstring is released causing very large torsional and bending vibrations. The similarity between the TOB time history presented in Figure 4 and the field data observed by Halsey *et al.* [10] is remarkable. Therefore, the proposed model seems to represent the stick–slip behavior quite well. In addition, since the model includes the coupling between the torsional and bending vibrations, the effect of torsional vibrations are clearly seen on the bending vibrations (Figures 5 and 6). The stick–slip oscillations are the main reasons for large lateral amplitudes and the complicated trajectory of the collars. The effect of bending vibrations on the torsional motion, however, is not as significant in this case since there are no impacts

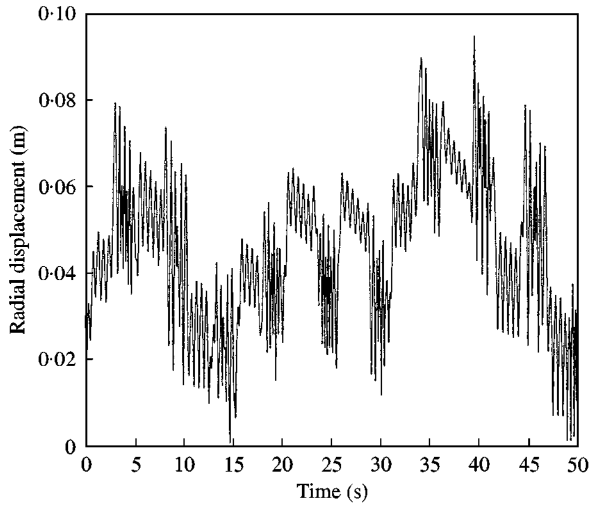

Figure 5. Effect of stick–slip oscillations on the lateral motion.

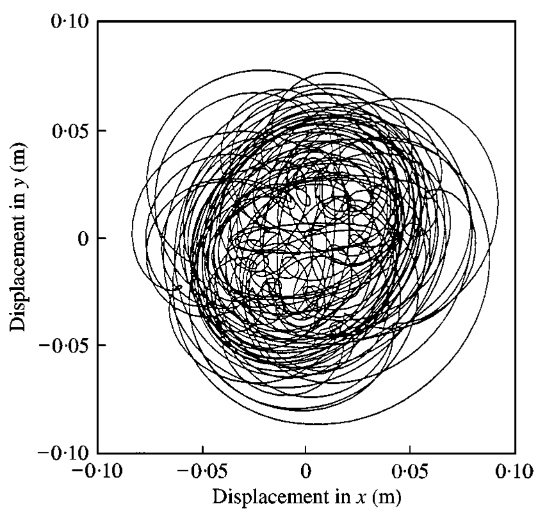

Figure 6. The trajectory of the geometric center of the drill collar section in the case of stick–slip oscillations.

with the borehole wall. Clearly, the presence of impacts will cause more significant interaction between lateral and torsional motions.

Generally, it has been demonstrated that increasing the rotary speed beyond a threshold value results in smoother drilling with respect to stick–slip oscillations [13]. However, high speeds may cause problems in the lateral motion such as whirling and parametric resonance. Therefore, it is of interest to find ways to increase the range of speeds at which smooth drilling is possible. An active control system is known to offer such a solution [10–14].

The control design for the system is carried out by solving equation (38). The state weighting matrix $\mathbf{Q}$ is taken as an identity matrix and $r = 0{\cdot}01$. The resulting gains are

$$\mathbf{K} = [-15 \;\; 10 \;\; 1{\cdot}6 \;\; 2{\cdot}7 \;\; 0{\cdot}013]. \tag{41}$$

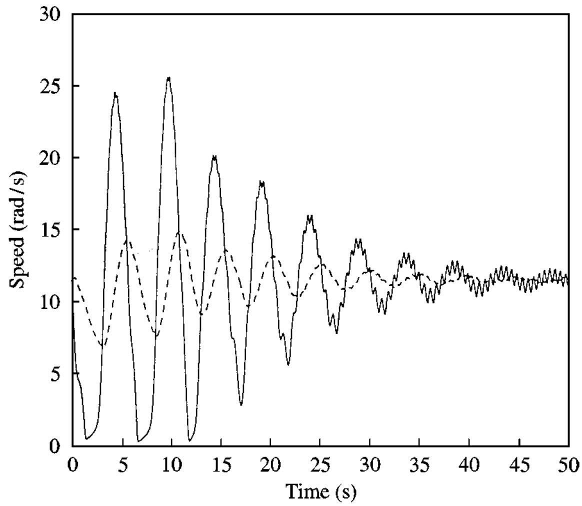

Figure 7. Effect of control on the bit and table speeds; key as Figure 3.

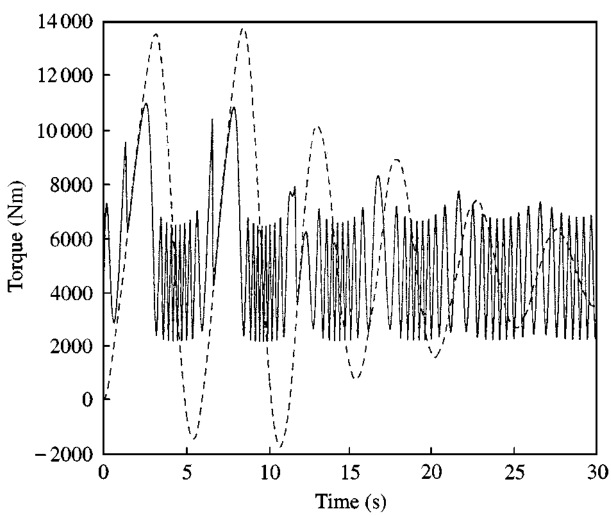

Figure 8. Effect of control on the bit and top torques; key as Figure 4.

When these gains are used the linear model yields the following closed-loop eigenvalues: $2{\cdot}03 \pm 15{\cdot}4i$, $-0{\cdot}183 \pm 1{\cdot}3i$, and $-0{\cdot}22$. The settling time for the dominant poles is about 25 s. Though the control is applied to the full non-linear model, these values can still give an idea about the performance of the controller. For instance, it is expected that this particular set of gains should suppress the vibrations within 25 s. A different set of weights will certainly result in a different performance. For instance, decreasing r improves the settling time (i.e., faster response).

Figures 7–10 show the response with the proposed controller when the desired rotary speed is selected as 11·6 rad/s. As can be seen in Figure 7, the controller is able to eliminate stick–slip vibrations within 30 s. This is in agreement with the settling time of the linear

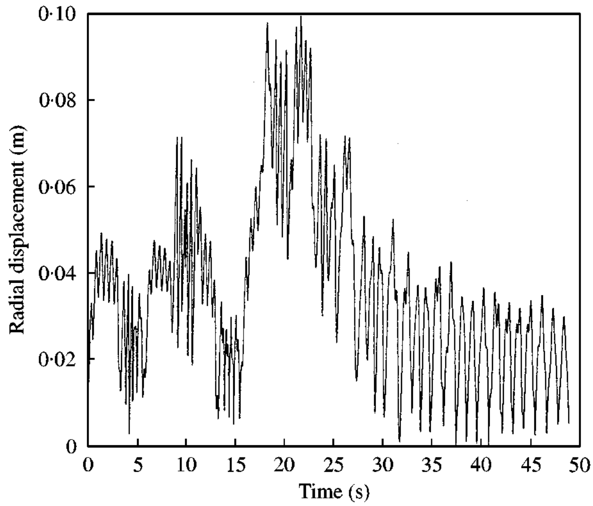

Figure 9. Effect of control on the lateral vibrations.

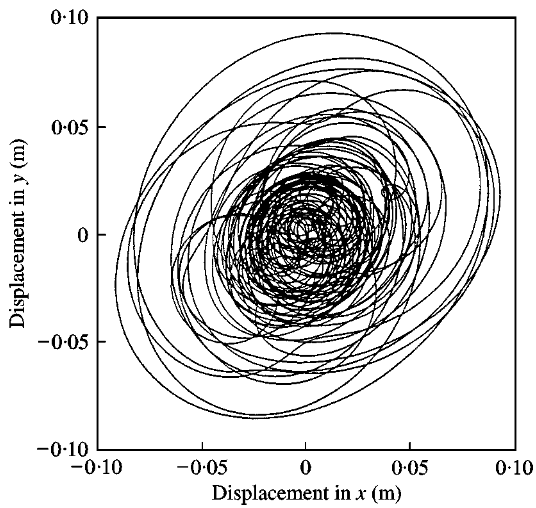

Figure 10. The trajectory of the geometric center of the drill collar section in the controlled drillstring.

model. Even during the transient, peak bit speeds are reduced compared to open-loop response. Also, the peak torques on the drillpipe are reduced. The effect on the bending vibrations during the transient is more complicated since there are few impacts of the collars with the borehole wall in the controlled drillstring (see Figure 9). The nature of the growth in the lateral vibrations suggest some form of transient instability which may be caused by a momentary parametric resonance. After the transient, however, the lateral vibrations are also reduced to the steady state whirling amplitudes. In any case, this simulation shows that the transient response with respect to both torsional and bending vibrations should be investigated before making a positive decision about a particular operating condition (i.e., desired r.p.m., and controller gains). Finally, Figures 11 and 12 compare the open- and

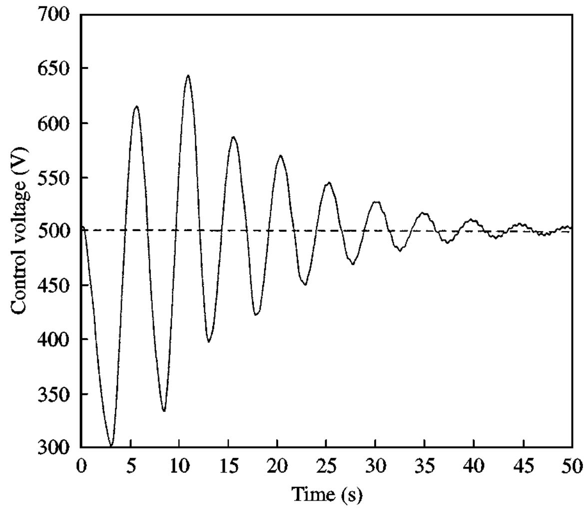

Figure 11. Comparison of the control effort for open- and closed-loop control: ——, closed loop; – – –, open loop.

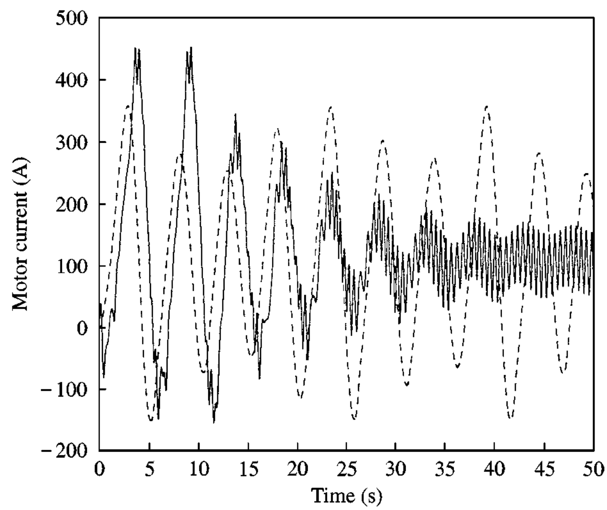

Figure 12. Comparison of the armature current for open- and closed-loop control; key as Figure 11.

closed-loop systems with respect to the control voltage and the motor current for this operating condition. It appears that the closed-loop system does not require excessive control effort when compared to the open-loop system. Therefore, the proposed control can easily be implemented using the existing DC motors in the drilling rig.

Clearly, the choice of the desired rotary table speed influences the system response. Figures 13–15 show the response with the same controller gains when the desired speed is selected as 15 rad/s. The problem of stick–slip at the speed is less, and therefore, the controller performance is superior. It is expected that this operating condition to result in a smoother drilling. On the other hand, reducing the desired rotary speed increases the effect of stick–slip, and it may be necessary to re-design the controller with a new set of

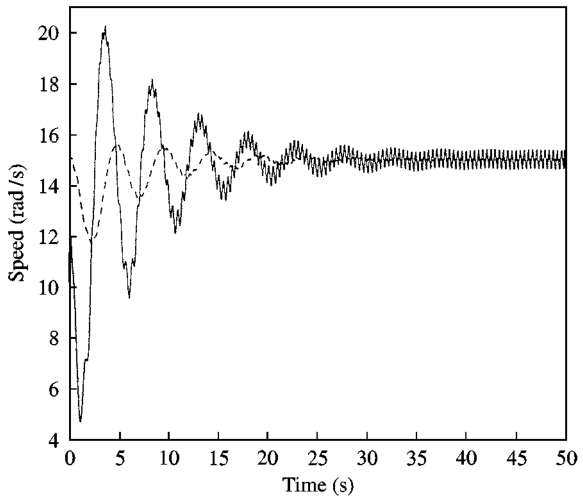

Figure 13. Effect of control on the bit and table speeds in the case of a higher table speed ($\omega_d = 15$ rad/s); key as Figure 3.

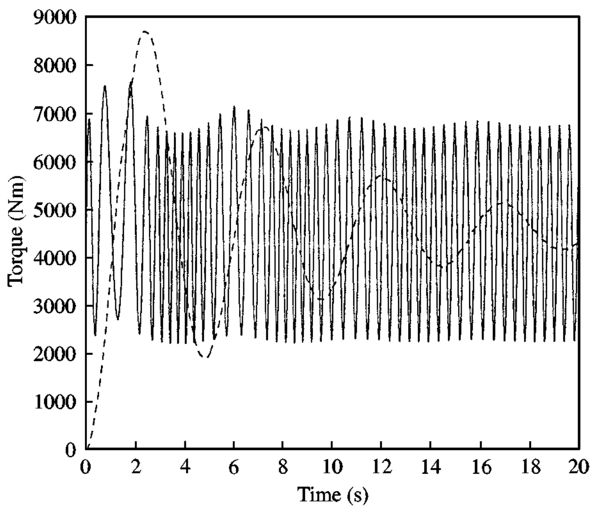

Figure 14. Effect of control on the bit and top torques in the case of a higher table speed ($\omega_d = 15$ rad/s); key as Figure 4.

tuning parameters Q and r. Simulations can easily be carried out on a PC at the rig, and suitable operating conditions can be obtained for efficient drilling.

6. CONCLUSIONS

A study of the coupled torsional and bending vibrations of an actively controlled drillstring has been presented. The proposed dynamic model includes the mutual dependence of torsional and bending vibrations. Furthermore, the bit/formation and drillstring/borehole wall interactions are assumed to be related to drillstring torsional and

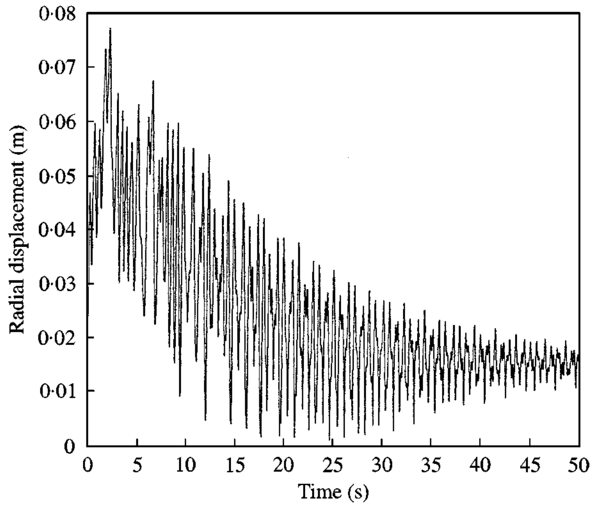

Figure 15. Effect of control on the lateral vibrations in the case of a higher table speed ($\omega_d = 15$ rad/s).

lateral motions. Simulation results are in close qualitative agreement with field observations regarding stick–slip oscillations. These vibrations are self-excited, and they generally disappear as the rotary table speed is increased beyond a threshold value. However, since increasing the rotary speed may cause lateral problems such as backward and forward whirling, impacts with the borehole wall, and parametric instabilities it is desirable to extend the range of safe drilling speeds. An optimal state feedback control has been designed to control the drillstring rotational motion. It has been shown that the proposed control can be effective in suppressing stick–slip oscillations once they are initiated. Therefore, it is possible to drill at lower speeds which are otherwise not possible without active control. However, the effect of control on the lateral vibrations may be significant and care must be taken in selecting a set of operating parameters.

ACKNOWLEDGEMENT

The first author acknowledges the support of Kuwait University, Research Administration, under Grant No. EM-122.

REFERENCES

1. J. D. Jansen 1991 *Journal of Sound and Vibration* **147**, 115–135. Non-linear rotor dynamics as applied to oilwell drillstring vibrations.
2. T. V. Aarrestad and A. Kyllingstad 1988 *Society of Petroleum Engineers Drilling Engineering* **3**, 12–18. An experimental and theoretical study of a coupling mechanism between longitudinal and torsional drillstring vibrations at the bit.
3. J. K. Vandiver, J. W. Nicholson and R. J. Shyu 1990 *Society of Petroleum Engineers Drilling Engineering* **5**, 282–290. Case studies of the bending vibration and whirling motion of drill collars.
4. G. F. Brett 1992 *Society of Petroleum Engineers Drilling Engineering* **7**, 168–174. The genesis of torsional drillstring vibrations.
5. V. A. Dunayevsky, F. Abbassian and A. Judzis 1993 *Society of Petroleum Engineers Drilling and Completion* **8**, 84–92. Dynamic stability of drillstrings under fluctuating weight on bit.

6. M. A. ELSAYED, D. W. DAREING and M. A. VONDERHEIDE 1997 *American Society of Mechanical Engineers Journal of Energy Resources Technology* **119**, 11–19. Effect of torsion on stability, dynamic forces, and vibration characteristics in drillstrings.
7. A. P. CHRISTOFOROU and A. S. YIGIT 1997 *Journal of Sound and Vibration* **206**, 243–260. Dynamic modelling of rotating drillstrings with borehole interactions.
8. S. J. KOTSONIS and P. D. SPANOS 1997 *Journal of Energy Resources Technology* **119**, 217–222. Chaotic and random whirling motion of drillstrings.
9. A. KYLLINGSTAD and G. W. HALSEY 1988 *Society of Petroleum Engineers Drilling Engineering* **3**, 369–373. A study of slip/stick motion of the bit.
10. G. W. HALSEY, A. KYLLINGSTAD and A. KYLLING 1988 *Proceedings 63rd Society of Petroleum Engineers Drilling Engineering Annual Technical Conference and Exhibition, Houston TX*, 277–282. Torque feedback used to cure slip–stick motion.
11. P. SANANIKONE, O. KOMOSHIMA and D. B. WHITE 1992 *Proceedings IADC/SPE Drilling Conference, New Orleans, LA*, 443–452. A field method for controlling drillstring torsional vibrations.
12. J. D. JANSEN, L. VAN DEN STEEN and E. ZACHARIASEN 1995 *SPE Drilling and Completion* **10** 250–254. Active damping of torsional drillstring vibrations with a hydraulic top drive.
13. J. D. JANSEN and L. VAN DEN STEEN 1995 *Journal of Sound and Vibration* **179**, 647–668. Active damping of self-excited torsional vibrations in oil well drillstring.
14. A. F. A. SERRARENS, M. J. G. VAN DE MOLENGRAFT, J. J. KOK and L. VAN DEN STEEN 1998 *IEEE Control System Magazine*, 19–30. H_∞ Control for suppressing stick–slip in oil well drillstrings.
15. W. D. ALDRED and M. C. SHEPPARD 1992 *Proceedings of 67th Annual Technical Conference and Exhibition, Washington, DC*, SPE Paper No. 24582. Drillstring vibrations: a new generation mechanism and control strategies.
16. A. S. YIGIT and A. P. CHRISTOFOROU 1998 *Journal of Sound and Vibration* **215**, 167–181. Coupled torsional and bending vibrations of drillstring subject to impact with friction.
17. R. W. TUCKER and C. WANG 1997 http://www.lancs.ac.uk/users/SPC/Physics.htm. The excitation and control of torsional slip–stick in the presence of axial vibrations.
18. Y. A. KHULIEF and A. A. SHABANA 1986 *Journal of Sound and Vibration* **104**, 187–207. Impact responses of multi-body systems with consistent and lumped masses.
19. Y. Wang and M. T. MASON 1992 *American Society of Mechanical Engineers Journal of Applied Mechanics* **59**, 635–642. Two-dimensional rigid-body collisions with friction.
20. A. E. BRYSON and Y. C. HO 1975 *Applied Optimal Control*. New York: John Wiley.